Desalination and Water Treatment
www.deswater.com
doi: 10.5004/dwt.2023.29291

284 (2023) 165–174
February

Synthesis and characterization of geopolymer foams from mineral wastes: application as adsorbent for Cu(II) and Pb(II) ions from aqueous solutions

Assia Ben Amor[a,e,*], Abdelkader Ouakouak[b,c], Sabrine Boucetta[d], Khaled Mahmoudi[e], Noureddine Hamdi[a,e]

[a]*Higher Institute of Water Sciences and Techniques, University of Gabès, Zrig 6072, Tunisia, Tel.: +216 24 617221; email: assia.benamor123@gmail.com (A.B. Amor), Tel.: +216 97 598 648; email: hamdinoureddine@yahoo.fr (N. Hamdi)*
[b]*Research Laboratory in Subterranean and Surface Hydraulics, University of Biskra, P.O. Box: 145 RP, Biskra 07000, Algeria, Tel.: +213 663 778 295; email: ouakouakk@yahoo.fr*
[c]*Hydraulic and Civil Engineering Department, University of El Oued, P.O. Box: 789, El Oued 39000, Algeria*
[d]*Laboratory of Ecobiology of Marine and Coastal Environments (EMMAL), Badji Mokhtar Annaba University, Algeria, Tel.: +213 791 914 164; email: sabrine.boucetta@yahoo.com*
[e]*Laboratoire des Matériaux Composites et Matériaux Argileux, CNRSM, Technopole Borj Cedria B.P. 73, 8027 Soliman, Tunisia, Tel.: +216 22 593 875; email: mahmoudikhaled1984@gmail.com*

Received 18 May 2022; Accepted 9 January 2023

ABSTRACT

Urban and industrial effluents are responsible for pollutant of which organic, mineral or physical nature. This gives these effluents aggressive and harmful character for the ecosystem and water resources. This work focuses on developing a porous geopolymeric materials as a low-cost, non-toxicity, and easy synthesis adsorbent for removing toxic metals from water. Brick waste and phosphogypsum were used as aluminosilicate raw materials for the synthesis of geopolymers. The silica fume was used as a blowing agent. The prepared geopolymers were characterized by Fourier-transform infrared spectroscopy and X-ray diffraction analysis technics, and were used to investigate the adsorption of Cu(II) and Pb(II) ions in the batch mode. Results show that the studied materials are rich mainly of quartz, cristobalite, and mullite. Adsorption experiments indicate that the equilibrium of Cu(II) and Pb(II) ions uptake can be reached at approximately 120 min (pH 5.0). The maximum removal efficiency of Cu(II) and Pb(II) observed was 55.55 and 83.33 $mg \cdot g^{-1}$, respectively for geo-M_2Na_{10} (waste brick + phosphogypsum + silica fume + NaOH) sample. The studied geopolymers exhibit a high adsorption capacity for Cu(II) and Pb(II) at initial concentration ranging from 50 to 400 $mg \cdot L^{-1}$. It was also found that the kinetic data are perfectly flow the pseudo-second-order model. The isotherm data of Cu(II) and Pb(II) adsorption onto the prepared adsorbents obeyed to the Langmuir model.

Keywords: Porous geopolymer; Heavy metals; Adsorption; Kinetic; Isotherm

1. Introduction

Geopolymers are solid/amorphous, which are synthesized from alkali activation of an aluminosilicate material [1], and appear as a potential alternative to the conventional cement materials. Geopolymers have been used in different applications, most of them are for the automotive and aerospace industries, non-ferrous foundries and metallurgy, civil engineering, cements and concretes, ceramics and plastics industries, waste management and wastewater treatment [2,3].

* Corresponding author.

Presented at the First International Seminar on Pollution, Health, Environment and Biomonitoring (SIPSEB-2021), 27–28 December 2021, Virtual Seminar, Skikda, Algeria

Many techniques based on chemical precipitation, reverse osmosis, electrochemical processes, ion exchange [4], coagulation [5] and adsorption [6] have been investigated to remove pollutants from water media. Currently, geopolymers have attracted much attention as new heavy metal adsorption ability [7].

Porous materials are reported to be efficient and low-cost adsorbents for organic and inorganic pollutants. Inorganic porous materials are generally studied in the developing of high-efficiency adsorption materials [8]. Ion-exchange properties shown by these materials are consequent to their unique crystalline microporous structure, identified by fixed pore dimensions that make them selectively accessible to metal ions, depending on their charge and size [9,10].

Bai and al. Have been used monolithic foamed geopolymers for extracting copper and ammonium, 87% removal for copper and 95% for ammonium, corresponding to an remove of 0.54 and 0.57 $mg \cdot g^{-1}$, respectively [11]. Another stimulating procedure has been reported by Tang et al. [12] on the use of metakaolin based geopolymer spheres. The spheres affinity about Cu^{2+}, Pb^{2+} and Ca^{2+} was demonstrated, with uptake values being 35, 46 and 24 $mg \cdot g^{-1}$, respectively. Several studies have been performed, and it has been revealed that the efficiency of the additive powder can be significantly modified through its composition with other materials [13].

The geopolymer foams were widely prepared from industrial wastes and their potential as a low-cost adsorbent for pollutants in water was reported in the existing literature [14]. Industrial waste recycling can decrease the need for natural resources and energy, and the interest from these recycled materials is to improve the performance of prepared geopolymer binders [15]. Waste brick and phosphogypsum are industrial by-products to get rid of, it's necessary a lot of money and great effort. Their potential use in the produce of geopolymer provides several benefits as are the saving use of natural resources then the solid by-product waste management [16].

In this work, the possibility of using phosphogypsum (PG) and waste brick (WB) as raw materials to produce geopolymer binders was investigated, and its ability to remove of Cu(II) and Pb(II) ions from water media. The geopolymerization method was applied to synthesize the phosphogypsum (PG) and waste brick (WB)-based geopolymer, the silica fume as a blowing agent and were activated by NaOH or KOH solution.

The prepared geopolymers samples were characterized by X-ray diffraction (XRD) and Fourier-transform infrared spectroscopy (FTIR), and then used as adsorbent to remove Cu(II) and Pb(II) from water. The adsorption behavior (performance and mechanisms) of Cu(II) and Pb(II) ions by using foams geopolymer was studied via batch experiments. In addition, different kinetic and equilibrium models were used to analyze the experimental data and understanding the adsorption properties of Cu(II) and Pb(II) onto the prepared materials.

2. Material and methods

2.1. Raw materials

The preparation of the geopolymers consists of mixing the raw material powder with solutions of alkali hydroxide, NaOH or KOH. In this research, we prepared porous geopolymer obtained from construction waste materials (brick powder (WB)), as well as industrial waste material (the phosphogypsum (PG), the silica fume (SF)), used as a heavy metal's adsorbent.

2.1.1. Waste brick (WB)

WB was available at the brick industry of Medenine (south of Tunisia). The chemical composition of the solid precursors indicated that the waste brick had a high content of SiO_2 (61.73%) compared to the Al_2O_3 (13.56%). Value of the mass ratio SiO_2/Al_2O_3 classifies the waste bricks as a siliceous material [17]. The WB was crushed and grounded using a crusher and a ball mill, then were sieved through 150 mm sieve.

2.1.2. Phosphogypsum (PG)

The PG was obtained from the chemical industry of Gabes city (south of Tunisia). The PG powder was washed with fresh water (until pH = 4) and dried at 100°C for a night and then were crushed in a mortar and then sieved through 150 mm sieve.

2.1.3. Alkali-activators

Generally, utilization of hydroxides of any alkalis such as sodium, potassium, calcium, lithium and silicates of sodium and potassium are suitable for activation of waste materials. However, most of researchers have used sodium and potassium-based alkali-activators to form alkali-activated bricks [18].

The alkaline activators used in the preparation of geopolymer are NaOH and KOH solutions. The solution was obtained by dissolving sodium or potassium hydroxide pellets in distilled water and allowed to cool to room temperature. The mixtures were obtained by hand mixing for 5 min.

The sodium hydroxide and potassium hydroxide solution were prepared with a concentration of 10, 12 and 14 M from solid NaOH or KOH capsules of 98% purity.

2.2. Geopolymer synthesis

Mixtures of the solid material powder with solutions of alkali hydroxide were established. Geopolymers were prepared from waste brick, washed and sieved phosphogypsum, the silica fume and alkaline liquid. The mixture was homogenized for 5 min. The paste samples were cast in cylindrical plastic molds with a diameter of 20 mm and height of 40 mm and vibrated to remove entrapped air. Then, it was heated at 65°C during 3 d (Fig. 1).

Samples were prepared by two types of mixtures (Table 1):

- –60% WB, 15% SF and 25% alkaline liquid.
- –40% WB, 15% SF, 20% PG and 25% alkaline liquid.

2.3. Chemicals

The pollutants elements studied in this work were Cu(II) and Pb(II). Solutions containing copper and lead cations

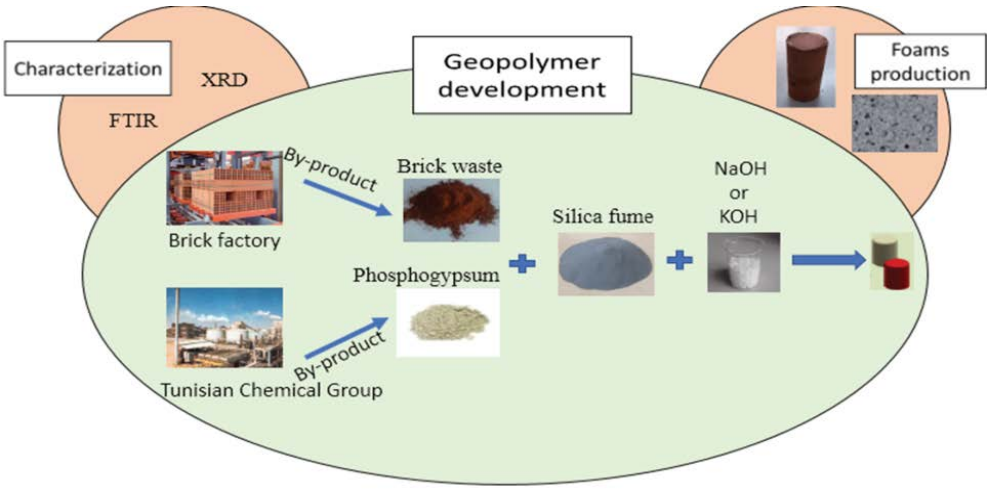

Fig. 1. Synthesis protocol of waste materials based geopolymer.

Table 1
Composition of the prepared geopolymers samples

Samples	WB (%)	SF (%)	PG (%)	NaOH (mol)	KOH (mol)
geo-M_1Na_{10}	60	15	–	10	–
geo-M_1Na_{12}	60	15	–	12	–
geo-M_1Na_{14}	60	15	–	14	–
geo-M_1k_{10}	60	15	–	–	10
geo-M_1k_{12}	60	15	–	–	12
geo-M_1k_{14}	60	15	–	–	14
geo-M_2Na_{10}	40	15	20	10	–
geo-M_2Na_{12}	40	15	20	12	–
geo-M_2Na_{14}	40	15	20	14	–
geo-M_2K_{10}	40	15	20	–	10
geo-M_2K_{12}	40	15	20	–	12
geo-M_2K_{14}	40	15	20	–	14

were prepared by dissolving copper(II) chloride $CuCl_2$ and lead(II) nitrate $Pb(NO_3)_2$ in deionized water, respectively.

2.4. Characterization methods

The waste materials and prepared geopolymers were characterized by FTIR and XRD analysis technics. The mineral crystalline phases of materials were determined by X-ray diffractometry using a PANalytical X'Pert-V diffractometer, which functions by reflection of Cu ka radiation (30 mA and 40 kV) of 5°/min scanning speed. The FTIR spectrum was recorded on a KBr disk, which contains 1% sample by mass, using a PerkinElmer (model783) spectrophotometer.

2.5. Batch adsorption studies

The adsorption experiments were performed according to the batch system at 25°C. The concentration of the aqueous solutions containing Cu^{2+} and Pb^{2+} was varied in the range of 50–400 mg·L^{-1}. The pH of solutions was controlled with adding a drops of HCl 0.1 M or NaOH 0.1 M for each adsorption test. Therefore 0.1 mg of geopolymer powder was added in 100 mL of the metal solution. Then after adsorption test, the residual concentrations of metal were determined by the atomic absorption spectrometer (AAS vario 6, Analytik Jena).

The differences in metal ion concentration were represented as the extraction of metal ion by the porous geopolymer adsorbent, according to Eq. (1):

$$Q_{ads} = \frac{(C_0 - C_t)V}{M} \quad (1)$$

Where C_0 and C_t (mg·L^{-1}) are the initial and at any time t concentrations of metal, respectively, V (L) is the volume, and M (g) is the weight of the adsorbent.

2.6. Theoretical foundation of kinetic and isotherm adsorption modeling

In the literature, many theoretical models are utilized to fit the adsorption kinetics and adsorption isotherm data. In this paper, the kinetics data was investigated using two models (the first-order and second-order). The two used isotherm models (Langmuir and Freundlich) were employed to describe the equilibrium data.

The adsorption efficiency of Cu(II) and Pb(II) ions was studied as a function of stirring time. The experimental data were fitted to the pseudo-first-order (2) [19] and the pseudo-second-order (2) [20] kinetic models.

- Pseudo-first-order:

$$q_t = q_e\left(1 - e^{-K_1 t}\right) \quad (2)$$

- Pseudo-second-order:

$$q_t = \frac{q_e^2 k_2 t}{1 + q_e k_2 t} \quad (3)$$

The equilibrium study was performed to understand the mechanism of Cu(II) and Pb(II) adsorption onto geopolymer foams. The non-linear forms of Langmuir [21] and Freundlich [22] models were used to fit data of adsorption isotherm.

- Langmuir

$$q_e = \frac{Q^0_{\max} K_L C_e}{1 + K_L C_e} \quad (4)$$

- Freundlich

$$q_e = K_F C_e^n \quad (5)$$

3. Results and discussion

3.1. Characterization of resultant mineral wastes based geopolymers

3.1.1. Chemical analysis

Table 2 presents the chemical analysis of the raw materials used in this study. Results of WB samples show that the SiO_2 is the major constituent and the loss on ignition is relatively lower. As for the PG sample, the main constituents are SO_3, CaO, and SiO_2.

3.1.2. XRD analysis

Data of the XRD analysis of WB and PG samples are presented in Fig. 2. The XRD diffractogram of PG sample reveals the presence mainly of gypsum and brushite, while the XRD of WB sample shows the presence specifically quartz and illite.

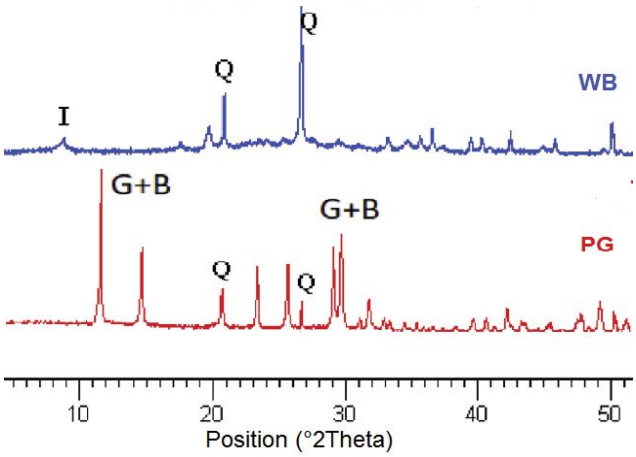

Fig. 2. XRD patterns of raw materials: WB and PG. G: gypsum; B: brushite; Q: quartz; I: illite.

3.1.3. FTIR analysis

Fig. 3 presents the FTIR spectra of WB and PG samples exposed to elevated temperature. The band characteristic of quartz (Si–O–Si vibrations) is located between 781 and 800 cm^{-1}. The band arising at ~1,660 cm^{-1} is due to the usual bending vibrations of water. The second vibration (~3,400 cm^{-1}) may be attributed to the hydrogen bonding of water molecules to the surface oxygen. As for the PG spectra, bands at 600 and 669 cm^{-1} are assigned to asymmetric vibration mode of SO_4. The stretching mode band was found at about 1,100 cm^{-1}.

Table 3 shows the properties of silica fume (SF) used in the preparation of porous geopolymers.

3.2. Characterization of geopolymer adsorbents

The prepared geopolymers were characterized by FTIR and XRD analysis technics.

3.2.1. XRD analysis

Results of Fig. 4 show that the studied materials are rich mainly of quartz, cristobalite and mullite. The XRD supported the amorphous features of the porous geopolymers.

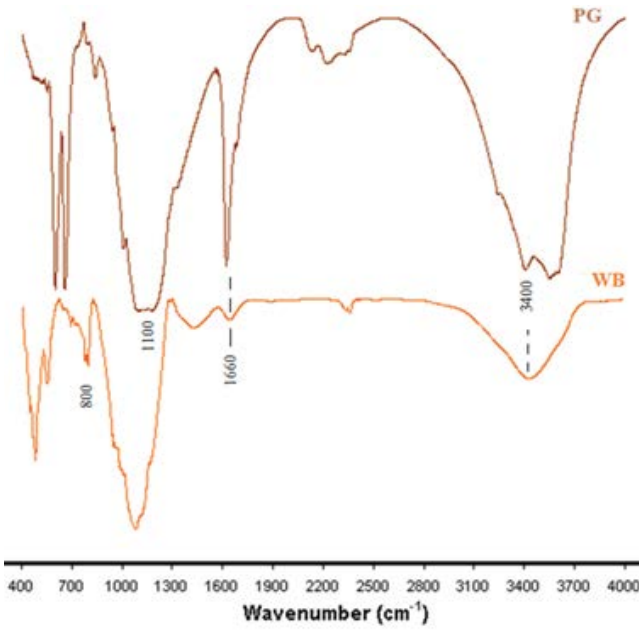

Fig. 3. Infrared spectra of raw materials (PG, WB).

Table 2
Chemical composition of the raw minerals geopolymer adsorbent

Oxides	SiO_2	Al_2O_3	Fe_2O_3	MgO	CaO	Na_2O	K_2O	SO_3	P_2O_5	LOI
WB	61.73	13.56	8.72	2.85	2.94	0.42	2.08	1.43	–	6.73
PG	10.32	1.54	0.21	0.64	24.56	0.98	0.45	41.12	1.43	18.31

Table 3
Technical properties of SF used

Appearance	Light grey powder
Bulk density	0.40 to 0.45
Real density (helium)	2.24
SiO_2 content	95%
Free C content	1.50%
Total S content 0.10%	0.10%
SiC content 1.50%	1.50%
Cl-content	0.06%
Oxide content (Fe, Al, Mg, Ca)	1.00%
Total alkali (Na_2O eq.)	0.60%
Specific surface BET ($m^2 \cdot g^{-1}$)	23

The crystalline phases were dissolved in the alkaline solution and the aluminosilicate by geopolymerization reaction [23]. The crystalline phase of the waste industrial powder is significantly modified into amorphous phase by means of the dissolution of crystalline particles in the alkaline solution during the geopolymerization reaction. In addition to that, the hump that appears at 20–35 is mainly related to N-A-S-H gel, and the size of amorphous humps is related to the amount of N-A-S-H gel synthesized [24]. The above results indicate that alkaline solution has a good decomposing effect on waste industrial particles.

3.2.2. FTIR analysis

FTIR spectra of elaborated matrix are depicted in Fig. 5. The FTIR bands are as follows:

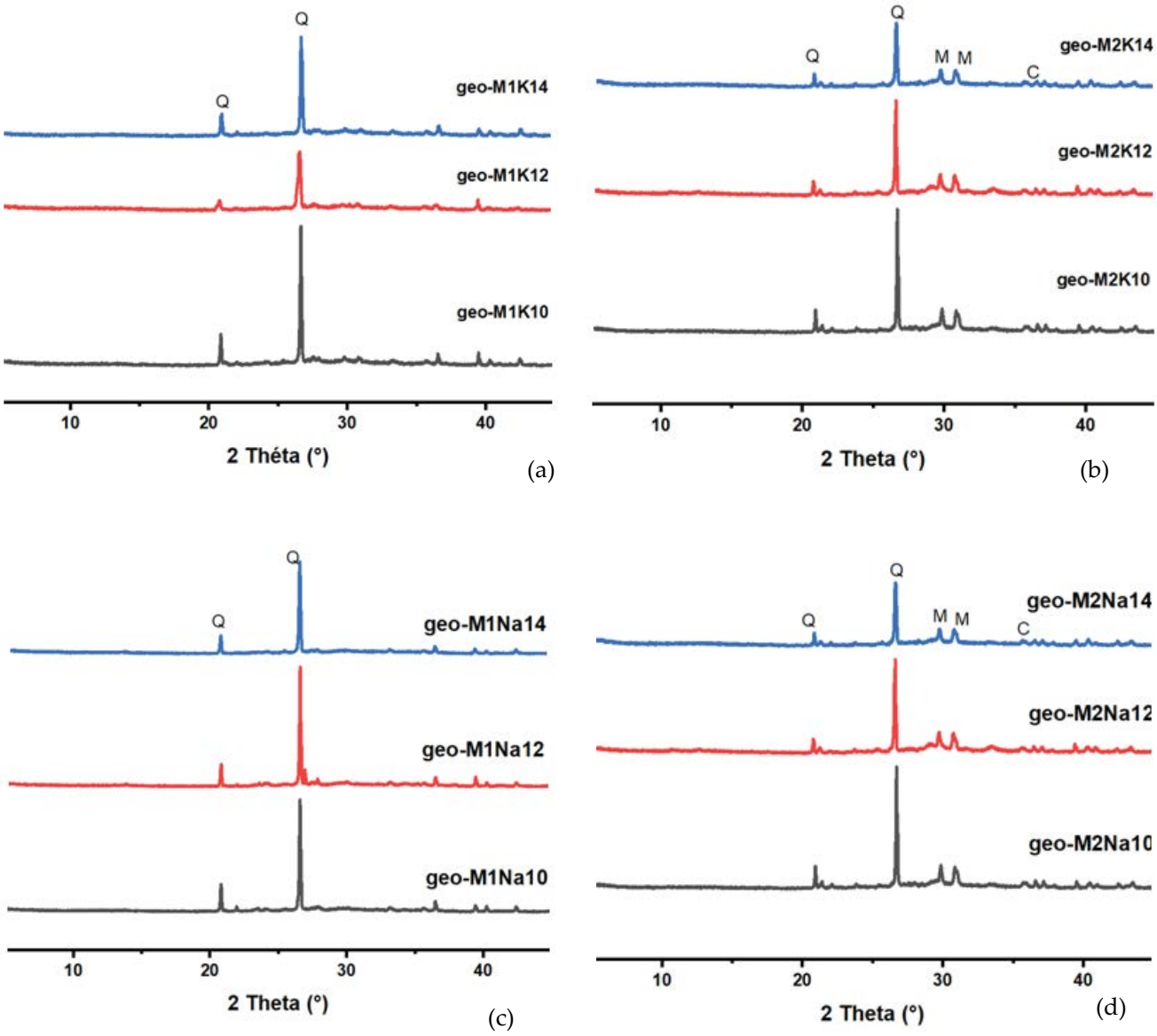

Fig. 4. XRD patterns of foamed geopolymers (a–d). Q: quartz; C: cristobalite; M: mullite.

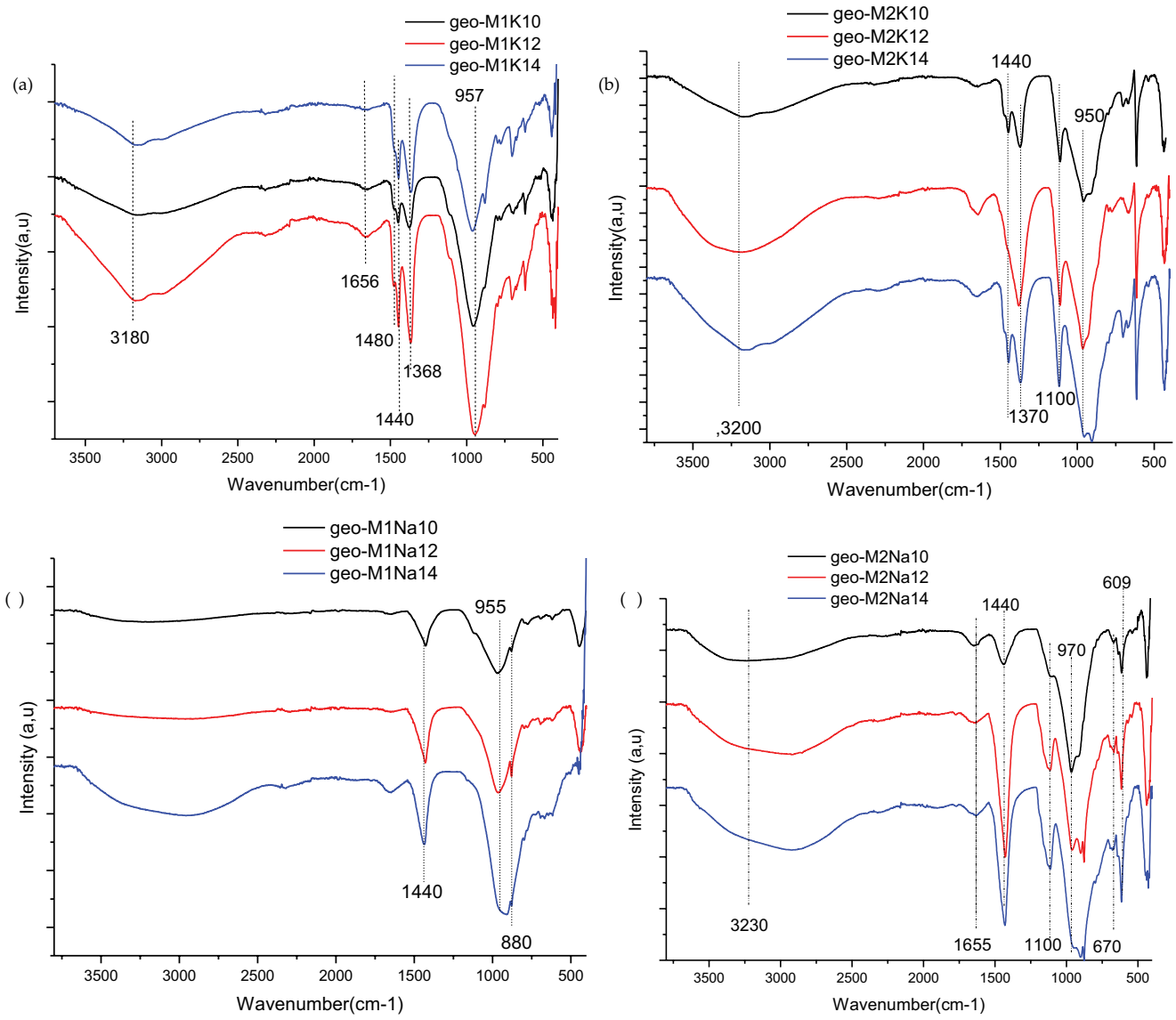

Fig. 5. FTIR spectra of foamed geopolymers (a–d).

- Stretching vibrations of O–H band of the kaolinite hydroxyl at 2,500–3,300 cm^{-1};
- Stretching vibrations of CO_2 located at around 1,440 cm^{-1};
- Asymmetric stretching vibration (T–O–Si) at 1,100–957 cm^{-1} where T = Si or Al;
- Stretching vibration of Si–O–Si in the region of 1,004–1,010 cm^{-1}.

The presence of the bands located at 670 and at 609 cm^{-1} are due to the quartz.

3.3. Sorption study of heavy metals

3.3.1. Effect of pH

The effect of pH on the adsorption of Cu(II) and Pb(II) ions is depicted in Fig. 6. The data reveal that the adsorption of both ions from their aqueous solution is significantly affected by the solution pH. The uptake ability of geopolymer was low at lower pH but increases as solution pH increases and found maximum at pH 5.0 for both ions. The adsorbed amount of Cu(II) and Pb(II) ions increased to reach 51 and 78 $mg \cdot g^{-1}$, respectively as solution pH 5.0.

3.3.2. Effect of contact time (Cu(II) and Pb(II) adsorption kinetics)

The effect of contact time of Cu(II) and Pb(II) ions solutions with geopolymers was assessed between 0 and 480 min, as given in Figs. 7 and 8. The results show a prompt uptake at first 60 min both of Cu(II) and Pb(II) ions. As contact time increased from 120 min, the adsorption efficiency for both metal ions increased and reached maximum value 52 $mg \cdot g^{-1}$ for Cu(II) and 79 $mg \cdot g^{-1}$ for Pb(II) ions for geo-M_2Na_{10} geopolymer.

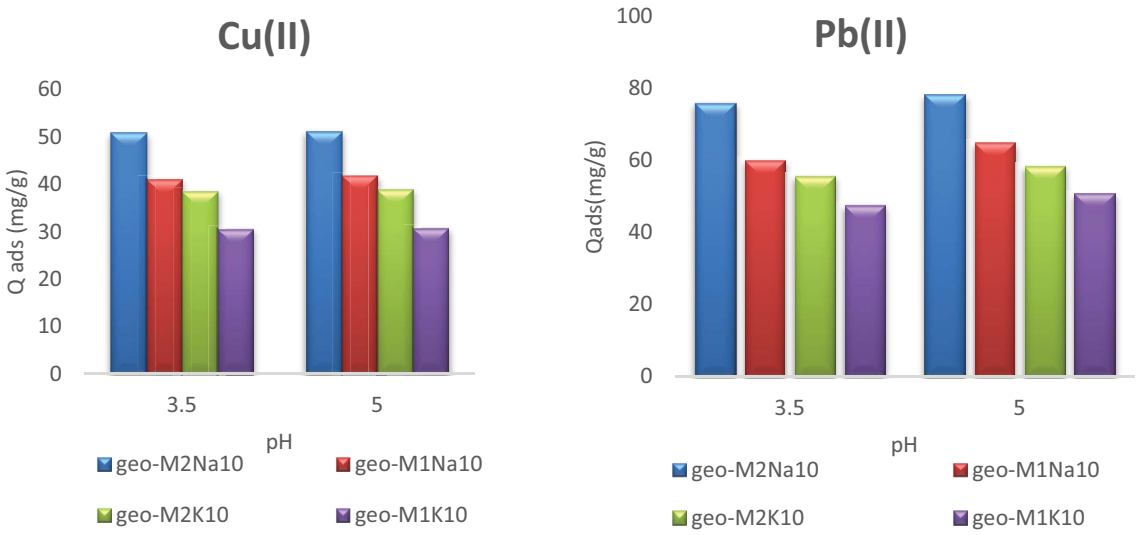

Fig. 6. Effect of pH value on the adsorption process of Cu(II) and Pb(II) onto geopolymers.

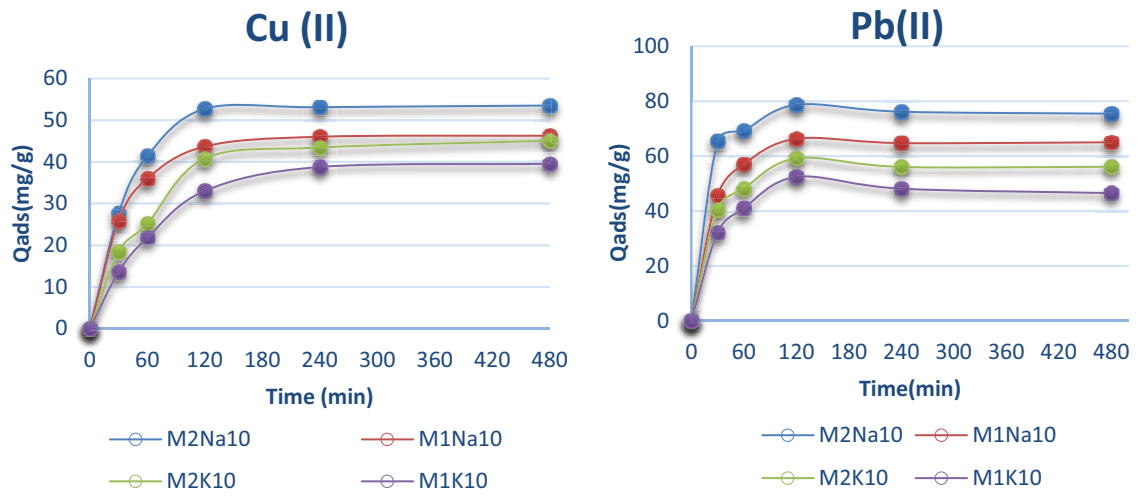

Fig. 7. Effect of contact time on the Cu(II) and Pb(II) adsorption onto geopolymers.

Fig. 8a–d of the modeling of kinetic data of copper and lead show that the pseudo-second-order equation well describes the experimental data compared to pseudo-first-order model. This finding is confirmed by the higher correlation value (R^2) and the less difference between the experimental and calculated q_e values in the case of pseudo-second-order (Tables 4 and 5).

3.3.3. Modeling of adsorption isotherm

To explore the interactions adsorbent–adsorbate involving adsorption, the isotherm data was obtained by varying the Cu(II) and Pb(II) initial concentration at a fixed constant dose of adsorbent. In this study, the nonlinear forms of Langmuir and Freundlich models were used to fit the equilibrium data.

From Fig. 9, the greater value of q_e indicates the accumulation of a greater number of ions to form a monosaturated layer. The results may be attributed to the presence of a greater number of active sites which enhance the removal ability of heavy metal by the adsorbent [25].

The correlation coefficient ($R^2 \approx 1$) values provided in Tables 6 and 7 are very close to one which describing that the experimental results have a strong association with the Langmuir isotherm. According to this model, the maximum adsorption capacity is 55.55 mg·g^{-1} for Cu(II) and 83.33 mg·g^{-1} for Pb(II).

3.3.4. Comparison with other adsorbents

To support the ability of the prepared geopolymer foams synthesized from mineral wastes as an effective adsorbent for copper and lead, the obtained adsorption capacity was compared to results of various adsorbents that have been reported in previous research in Table 8. It can be seen from data that the geopolymer prepared in this paper has nice adsorption effect.

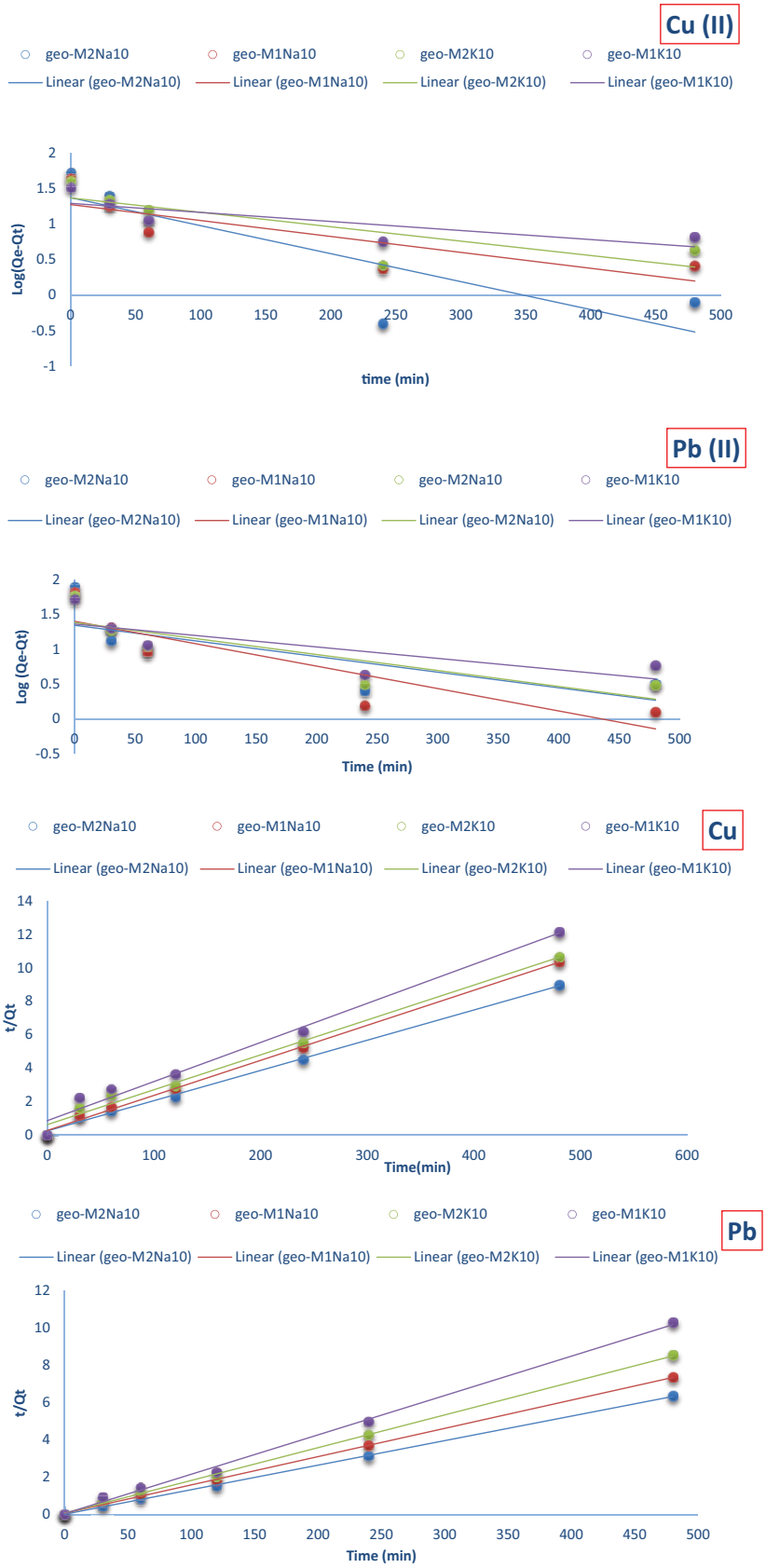

Fig. 8. (a) Kinetic pseudo-first-order of Cu(II) adsorption, (b) kinetic pseudo-second-order of Cu(II) adsorption, (c) kinetic pseudo-first-order of Pb(II) adsorption and (d) kinetic pseudo-second-order of Pb(II) adsorption.

Table 4
Relative kinetic parameters of pseudo-first-order and pseudo-second-order models for the Cu(II)

	Geopolymer	K ($L \cdot min^{-1}$)	q_e ($mg \cdot g^{-1}$)	R^2
Pseudo-first-order	geo-M_1K_{10}	0.005	25.110	0.870
	geo-M_2K_{10}	0.005	35.480	0.930
	geo-M_1Na_{10}	0.006	25.120	0.890
	geo-M_2Na_{10}	0.075	25.110	0.907
Pseudo-second-order	geo-M_1K_{10}	4.770	43.470	0.998
	geo-M_2K_{10}	5.500	48.300	0.994
	geo-M_1Na_{10}	0.010	50.000	0.994
	geo-M_2Na_{10}	0.001	55.550	0.999

Table 5
Relative kinetic parameters of pseudo-first-order and pseudo-second-order models for the Pb(II)

	Geopolymer	K ($L \cdot min^{-1}$)	q_e ($mg \cdot g^{-1}$)	R^2
Pseudo-first-order	geo-M_1K_{10}	0.011	42.270	0.550
	geo-M_2K_{10}	0.017	42.070	0.760
	geo-M_1Na_{10}	0.002	41.590	0.840
	geo-M_2Na_{10}	0.017	42.070	0.760
Pseudo-second-order	geo-M_1K_{10}	0.005	47.610	0.996
	geo-M_2K_{10}	0.002	58.820	0.998
	geo-M_1Na_{10}	0.001	66.660	0.999
	geo-M_2Na_{10}	0.005	76.33	0.999

Table 6
Isotherm constant parameters for the Cu(II) adsorption onto geopolymers

	Q_{max} ($mg \cdot g^{-1}$)	K_l	R^2
geo-M_1K_{10}	33.330	0.030	0.999
geo-M_2K_{10}	40.810	0.020	0.999
geo-M_1Na_{10}	50.000	0.020	0.999
geo-M_2Na_{10}	55.550	0.018	0.999
	$1/n$	K_F	R^2
geo-M_1K_{10}	0.069	24.500	0.890
geo-M_2K_{10}	0.013	36.500	0.170
geo-M_1Na_{10}	0.015	40.440	0.170
geo-M_2Na_{10}	0.046	40.400	0.564

Table 7
Isotherm constant parameters for the Pb(II) adsorption onto geopolymers

	$1/n$	K_F	R^2
geo-M_1K_{10}	0.102	25.533	0.719
geo-M_2K_{10}	0.015	38.474	0.173
geo-M_1Na_{10}	0.013	42.948	0.900
geo-M_2Na_{10}	0.060	48.424	0.890
	Q_{max} ($mg \cdot g^{-1}$)	K_l	R^2
geo-M_1K_{10}	54.050	0.012	0.999
geo-M_2K_{10}	61.720	0.014	0.999
geo-M_1Na_{10}	71.420	0.016	0.999
geo-M_2Na_{10}	83.330	0.018	0.999

Table 8
Adsorption results of Cu(II) and Pb(II) onto different adsorbents from literature reports

Adsorbent	Adsorbate	Adsorption capacity ($mg \cdot g^{-1}$)	References
Fly ash geopolymer	Cu(II)	90	[27]
Geopolymer/alginate hybrid		60.8	[28]
Geopolymer from metakaolin and biomass ash		58.824	[29]
CTAB modified geopolymers		40.00	[30]
Geopolymer foams from mineral wastes		55.55	This work
Waste concrete powder	Pb(II)	40.06	[31]
Geopolymer-alginate-chitosan composites		142.67	[32]
Metakaolin/slag based geopolymer		95.61	[7]
Geopolymer foams from mineral wastes		83.33	This work

4. Conclusion

In this study, porous geopolymers were prepared, characterized by FTIR and XRD analysis technics, and used as adsorbent. Batch experiments were conducted to investigate the removal of Cu(II) and Pb(II) at different conditions. Results show that the studied materials are rich mainly of quartz, cristobalite and mullite. Batch experiments indicate that the Cu(II) and Pb(II) ions adsorption equilibrium can be reached at approximately 120 min (pH 5.0). The maximum removal efficiency of Cu(II) and Pb(II) observed was 55.55 and 83.33 $mg \cdot g^{-1}$, respectively, for geo-M_2Na_{10} sample. The studied geopolymers exhibit a high adsorption capacity for Cu(II) and Pb(II) adsorption at initial concentration ranging from 50 to 400 $mg \cdot L^{-1}$. It was also found that the kinetic data are perfectly flow the pseudo-second-order model.

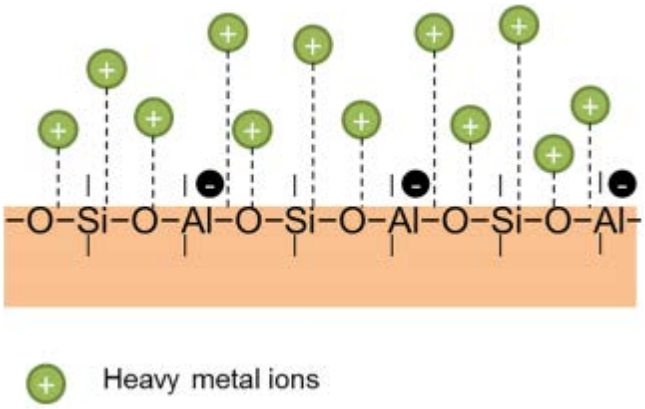

Fig. 9. Pictorial representation of the heavy metal attachment with geopolymer [26].

The isotherm data of Cu(II) and Pb(II) adsorption onto the prepared adsorbents obeyed to the Langmuir model.

References

[1] A. Maleki, Z. Hajizadeh, V. Sharifi, Z. Emdadi, A green, porous and eco-friendly magnetic geopolymer adsorbent for heavy metals removal from aqueous solutions, J. Cleaner Prod., 215 (2019) 1233–1245.
[2] F. Gouny, F. Fouchal, O. Pop, P. Maillard, S. Rossignol, Mechanical behavior of an assembly of wood-geopolymer-earth bricks, Constr. Build. Mater., 38 (2013) 110–118.
[3] X. Guo, H. Shi, W.A. Dick, Compressive strength and microstructural characteristics of class C fly ash geopolymer, Cem. Concr. Compos., 32 (2010) 142–147.
[4] Y. Li, X. Zeng, Y. Liu, S. Yan, Z. Hu, Y. Ni, Study on the treatment of copper-electroplating wastewater by chemical trapping and flocculation, Sep. Purif. Technol., 31 (2003) 91–95.
[5] M. Eloussaief, I. Jarraya, M. Benzina: Adsorption of copper ions on two clays from Tunisia: pH and temperature effects,. Appl. Clay Sci., 46 (2009) 409–413.
[6] N. Hamdi, I. Ben Messaoud, E. Srasra, Production of geopolymer binders using clay minerals and industrial wastes, C.R. Chim., 22 (2019) 220–226.
[7] X. Feng, S. Yan, S. Jiang, K. Huang, X. Ren, X. Du, P. Xing, Green synthesis of the metakaolin/slag based geopolymer for the effective removal of methylene blue and Pb(II), Silicon, 14 (2022) 6965–6979.
[8] F. Hoffmann, M. Cornelius, J. Morell, M. Fröba, Silica-based mesoporous organic–inorganic hybrid materials, Angew. Chem. Int. Ed., 45 (2006) 3216–3251.
[9] Breck, D.W. Zeolite, Molecular Sieves: Structure, Chemistry and Use, Wiley, New York, NY, USA, 1974.
[10] B. Liguori, P. Aprea, G. Roviello, C. Ferone, Self-supporting zeolites by geopolymer gel conversion, Microporous Mesoporous Mater., 286 (2019) 125–132.
[11] C. Bai, G. Franchin, H. Elsayed, A. Zaggia, L. Conte, H. Li, P. Colombo, High-porosity geopolymer foams with tailored porosity for thermal insulation and wastewater treatment, J. Mater. Res., 32 (2017) 3251–3259.
[12] Q. Tang, Y.-y. Ge, K.-t. Wang, Y. He, X.-m. Cui, Preparation and characterization of porous metakaolin-based inorganic polymer spheres as an adsorbent, Mater Des., 88 (2015) 1244–1249.
[13] J. Rahimi, R. Taheri-Ledari, M. Niksefat A. Maleki, Enhanced reduction of nitrobenzene derivatives: effective strategy executed by Fe_3O_4/PVA-10%Ag as a versatile hybrid nanocatalyst, Catal. Commun., 134 (2020) 105850, doi: 10.1016/j.catcom.2019.105850.
[14] A. Maleki, M. Mohammad, Z. Emdadi, N. Asim, M. Azizi, J. Safaei, Adsorbent materials based on a geopolymer paste for dye removal from aqueous solutions, Arabian J. Chem., 13 (2020) 3017–3025.
[15] C. Thormark, Conservation of energy and natural resources by recycling building waste, Resour. Conserv. Recycl., 33 (2001) 113–130.
[16] I. Ben Messaoud, N. Hamdi, E. Srasra, Physicochemical properties of geopolymer binders made from Tunisian clay, Mater. Focus, 7 (2018) 114–120
[17] E. Tiffo, A. Elimbi, J.D. Manga, A.B. Tchamba, Red ceramics produced from mixtures of kaolinite clay and waste glass, Braz. J. Sci. Technol., 2 (2015), doi: 10.1186/s40552-015-0009-9.
[18] C. Chen, Q. Li, L. Shen, J. Zhai, Feasibility of manufacturing geopolymer bricks using circulating fluidized bed combustion bottom ash, Environ. Technol., 33 (2012) 1313–1321.
[19] B.K.S.S. Langergren, Zurtheorie der sogenannten adsorption geloesterstoffe, Veternskapsakad Handlingar, 24 (1898) 1–39.
[20] Y.S. Ho, G. McKay, The sorption of lead(II) ions on peat, Water Res., 33 (1999) 578–584.
[21] I. Langmuir, The adsorption of gases on plane surfaces of glass, mica and platinum, J. Am. Chem. Soc., 40 (1918) 1361–1367.
[22] H.M.F. Freundlich, Uber die adsorption in losungen, Z. Phys. Chem., 57 (1906) 385–470.
[23] M. Jin, Z. Zheng, Y. Sun, L. Chen, Z. Jin, Resistance of metakaolin-MSWI fly ash based geopolymer to acid and alkaline environments, J. Non-Cryst. Solids, 450 (2016) 116–122.
[24] N. Hui-Teng, H. Cheng-Yong, L. Yun-Ming, M.M.A.B. Abdullah, K. Ern Hun, H.M. Razi, N. Yong-Sing, Formulation, mechanical properties and phase analysis of fly ash geopolymer with ladle furnace slag replacement, J. Mater. Res. Technol., 12 (2021) 1212–1226.
[25] A. Samant, B. Nayak, P.K. Misra, Kinetics, and mechanistic interpretation of fluoride removal by nanocrystalline hydroxyl apatite derived from *Limacine artica* shells, J. Environ. Chem. Eng., 5 (2017) 5429–5438.
[26] U. Ghani, S. Hussain, Noor-ul-Amin, M. Imtiaz, S. Ali Khan, Laterite clay-based geopolymer as a potential adsorbent for the heavy metals removal from aqueous solutions, J. Saudi Chem. Soc., 24 (2020) 874–884.
[27] S. Wang, L. Li, Z. Zhu, Solid-state conversion of fly ash to effective adsorbents for Cu removal from wastewater, J. Hazard. Mater., 139 (2007) 254–259.
[28] Y. Ge, X. Cui, C. Liao, Z. Li, Facile fabrication of green geopolymer/alginate hybrid spheres for efficient removal of Cu(II) in water: batch and column studies, Chem. Eng. J., 311 (2017) 126–134.
[29] A. Purbasari, I. Istadi, A. Kumoro, I. Sumantri, S. Silviana, Geopolymer from metakaolin and biomass ash for Cu(II) ions adsorption from aqueous solutions: kinetics and isotherm studies, J. Chem. Technol. Metall., 56 (2021) 1225–1233.
[30] A. Singhal, B.P. Gangwar, J.M. Gayathry, CTAB modified large surface area nanoporous geopolymer with high adsorption capacity for copper ion removal, Appl. Clay Sci., 150 (2017) 106–114.
[31] Z. Ma, R. Xue, J.S. Li, Y. Zhao, S.P. Chi, Use of thermally modified waste concrete powder for removal of Pb(II) from wastewater: effects and mechanism, Environ. Pollut., 277 (2021) 116776, doi: 10.1016/j.envpol.2021.116776.
[32] C. Yan, L. Guo, D. Ren, P. Duan, Novel composites based on geopolymer for removal of Pb(II), Mater. Lett., 239 (2019) 192–195.